

Supplementary Information

Mechanochemical coupling of two coupled kinesin monomers: comparison with that of the single dimer

Ping Xie

Supplementary text

The model for the mechanochemical coupling of the kinesin dimer

The model for the processive movement of the kinesin-1 dimer on MT is built up based mainly upon the following three elements [S1,S2]. (1) The variation of the interaction between a kinesin head and MT in an ATPase cycle is described in element (1) of the main text. (2) In ADP and ϕ states, the head has an open nucleotide-binding pocket (NBP) and the conformation, with its NL being unable to dock onto the head, as structural and experimental data showed [S3–S5], and the head having a high affinity to the partner ADP-head, as all-atom molecular dynamics (MD) simulations showed [S6]. In ATP and ADP.Pi states, NBP closing can occur, which is associated with a large conformational change of the head, so that the NL can dock onto the head, as structural and experimental data showed [S3–S5], and the affinity of the head to the partner ADP-head is reduced greatly, as all-atom MD simulations showed [S6]. When the NL is in the minus-ended direction, the interference of the NL prohibits the closing of NBP and thus the large conformational change of the ATP-head. (3) The NL-orientation dependent but force independent ATPase activity is described in element (3) of the main text.

The mechanochemical coupling pathway of the dimer at saturating ATP concentrations can be schematically shown in Fig. S1. We begin the pathway with the two heads in ATP state binding strongly to MT (Fig. S1a). The trailing ATP-head has a large conformational change relative to that in ADP and ϕ states, a closed NBP and a docked NL in the forward orientation, while the leading ATP-head with the NL in the backward orientation has no the large conformational change and an open NBP. ATP transition to ADP can take place independently in both heads, but with the trailing head of the NL in the forward orientation has a much higher rate of ATP transition to ADP than the leading head of the NL not in the forward orientation.

First, consider ATP transition to ADP taking place in the trailing head in Fig. S1a. By overcoming the very weak binding energy E_{w1} , the trailing head detaches readily from tubulin II and diffuses rapidly to the intermediate position relative to the MT-bound head, where the two heads have the high binding energy to each other (Fig. S1b). In the intermediate state, without the NL interference NBP closing together with the large conformational change of the MT-bound ATP-head take place rapidly (with rate $k_{NL} \gg k^{(+)}$), reducing greatly the binding energy between the two heads and inducing the NL docking of the MT-bound ATP-head

(Fig. S1c). Then, with probability P_{E2} , the detached ADP-head can diffuse forward and bind to the front tubulin IV with affinity E_{w2} (Fig. S1d). Stimulated by MT, ADP is released from the leading head, followed by ATP binding (Fig. S1e). In Fig. S1c, with probability $1-P_{E2}$, the detached ADP-head can also diffuse backward and bind to the previous tubulin II with affinity E_{w2} (noting that after the detachment of the ADP-head the affinity of tubulin II to ADP-head has transited from E_{w1} to E_{w2} in time t_r of the order of 10 μ s), followed by ADP release and then ATP binding (Fig. S1a). Note that the backward diffusion of the detached ADP-head and binding to the previous tubulin II (the transition from Fig. S1c to a) requires overcoming the energy barrier (E_0) associated with the large conformational change and NL docking of the MT-bound ATP-head. From Fig. S1a to e, the dimer moves forward by a step of size $d = 8$ nm, giving an effective mechanochemical coupling cycle. From Fig. S1a to c and returning to Fig. S1a, the dimer is not moved although an ATP is hydrolyzed, giving a futile mechanochemical coupling cycle.

Second, consider ATP transition to ADP taking place in the leading head in Fig. S1a. By overcoming the very weak binding energy E_{w1} , the leading head detaches from tubulin III and diffuses rapidly to the intermediate position relative to the MT-bound head (Fig. S1f). From the intermediate position, with probability $1-P_{E2}$, by overcoming the energy barrier E_0 the detached ADP-head can diffuse backward further and bind to tubulin I with affinity E_{w2} (Fig. S1g). Stimulated by MT, ADP is released from the trailing head, followed by ATP binding (Fig. S1h). From the intermediate position, with probability P_{E2} the detached ADP-head can also diffuse forward and bind to the previous tubulin III with affinity E_{w2} in time t_r , followed by ADP release and then ATP binding (Fig. S1a). From Fig. S1a to h, the dimer moves backward by a step of size d with the hydrolysis of an ATP. From Fig. S1a to f and returning to Fig. S1a, the dimer is not moved although an ATP is hydrolyzed.

As shown elsewhere [S1,S2,S7,S8,S11,S12], with the model shown in Fig. S1, the available single-molecule experimental data on diverse aspects of the dynamics of the kinesin dimer—such as the dependences of velocity, stepping ratio, randomness parameter, run length, dissociation rate, etc., on both forward and backward loads—can be reproduced quantitatively.

Supplementary references

- [S1] Xie P. (2021) Dynamics of kinesin motor proteins under longitudinal and sideways loads. *J. Theor. Biol.* 530, 110879.
- [S2] Xie P. (2023) Effect of the neck linker on processive stepping of kinesin motor. *Biophysica* 3, 46–68.
- [S3] Shang Z., Zhou K., Xu C., Csencsits R., Cochran J.C., Sindelar C.V. (2014) High-resolution structures of kinesin on microtubules provide a basis for nucleotide-gated force-generation. *eLife* 3, e04686.
- [S4] Rice S., Lin A.W., Safer D., Hart C.L., Naber N., Carragher B.O., Cain S.M., Pechatnikova E., Wilson-Kubalek E.M., Whittaker M., Pate E., Cooke R., Taylor E.W., Milligan R.A., Vale R.D. (1999) A structural change in the kinesin motor protein that drives motility. *Nature* 402, 778–784.
- [S5] Asenjo A.B., Weinberg Y., Sosa H. (2006) Nucleotide binding and hydrolysis induces a disorder-order transition in the kinesin neck-linker region. *Nat. Struc. Mol. Biol.* 13, 648–654.

- [S6] Shi X.-X., Guo S.-K., Wang P.-Y., Chen H., Xie P. (2020) All-atom molecular dynamics simulations reveal how kinesin transits from one-head-bound to two-heads-bound state. *Proteins* 88, 545–557.
- [S7] Guo S.-K., Wang P.-Y., Xie P. (2017) A model of processive movement of dimeric kinesin. *J. Theor. Biol.* 414, 62-75.
- [S8] Xie P., Guo S.-K., Chen H. (2019) A generalized kinetic model for coupling between stepping and ATP hydrolysis of kinesin molecular motors. *Int. J. Mol. Sci.* 20, 4911.
- [S9] Andreasson J.O.L., Shastry S., Hancock W.O., Block S.M. (2015). The mechanochemical cycle of mammalian kinesin-2 KIF3A/B under load. *Current Biology* 25, 1166-1175.
- [S10] Bensel B.M., Woody M.S., Pyrpassopoulos S., Goldman Y.E., Gilbert S.P., Ostap E.M. (2020) The mechanochemistry of the kinesin-2 KIF3AC heterodimer is related to strain-dependent kinetic properties of KIF3A and KIF3C. *Proc. Natl. Acad. Sci. U.S.A.* 117, 15632–15641.
- [S11] Xie P. (2020) Theoretical analysis of dynamics of kinesin molecular motors. *ACS Omega* 5, 5721–5730.
- [S12] Xie P. (2021) Insight into the chemomechanical coupling mechanism of kinesin molecular motors. *Commun. Theor. Phys.* 73, 57601.

Supplementary figures

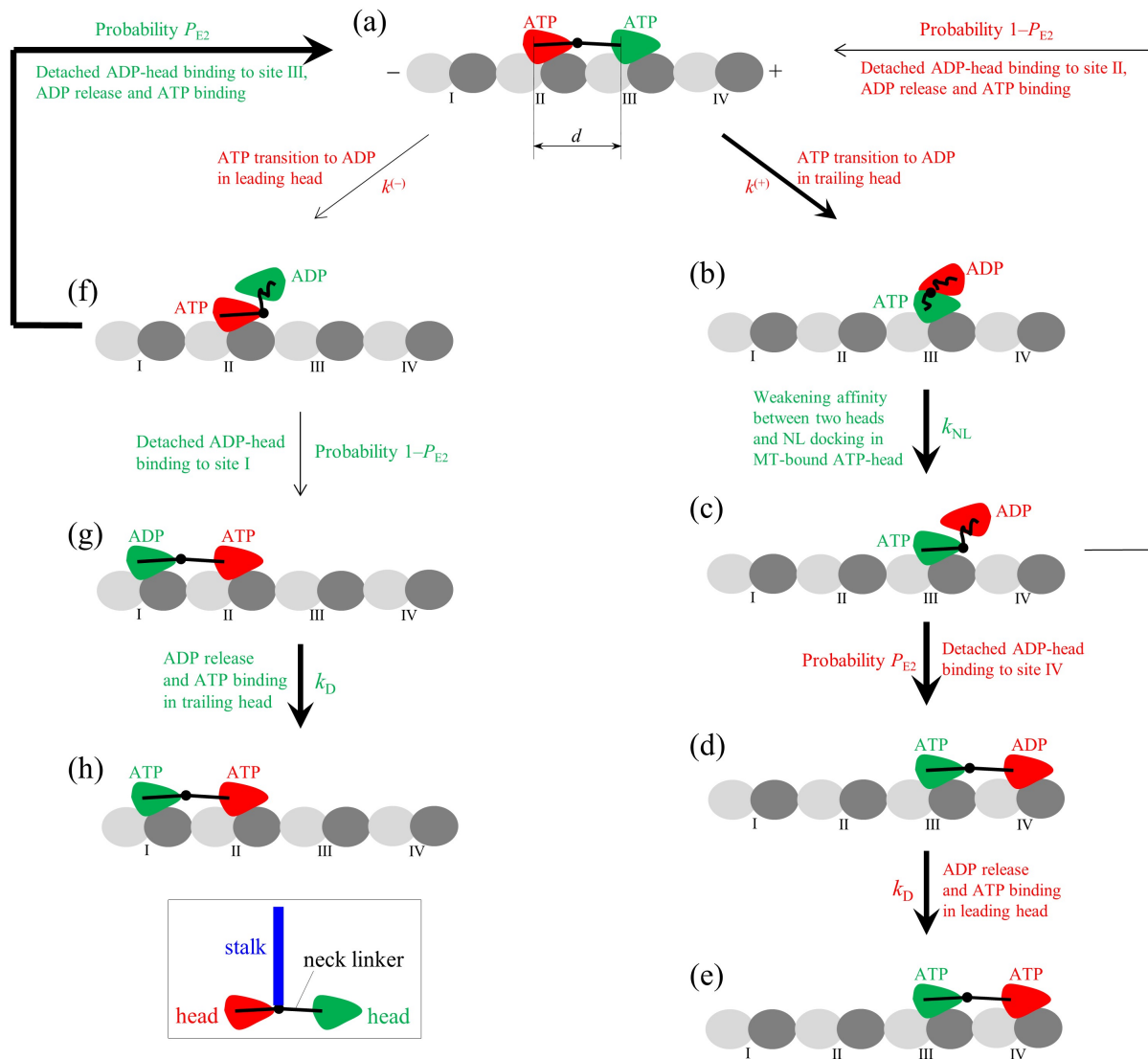


Fig. S1. Schematic illustration of the model for mechanochemical coupling of kinesin-1 dimer at saturating ATP concentrations. (a) – (h) The mechanochemical coupling pathway (see Supplementary text for detailed descriptions). The thickness of the arrow represents the relative magnitude of the probability of the transition between the two states connected by the arrow under no load. Since ATP-binding rate at saturating ATP is very large, the rate of ATP binding is not indicated here. Since ADP release from the MT-bound head is a non-rate-limiting step of the ATPase activity, it is considered here that ADP release from the leading ADP-head occurs before ATP transition to ADP in the trailing head. Since the diffusion of the head from the local tubulin to the intermediate position, which occurs after ATP transition to ADP in the head, and the diffusion of the detached head from the intermediate position to the nearest unoccupied tubulin, which occurs after the reduction of the affinity between the two head, are on the timescale of $1 \mu s$, which is much shorter than the rate constants of the ATPase activity, the rates of these diffusions are not indicated here.

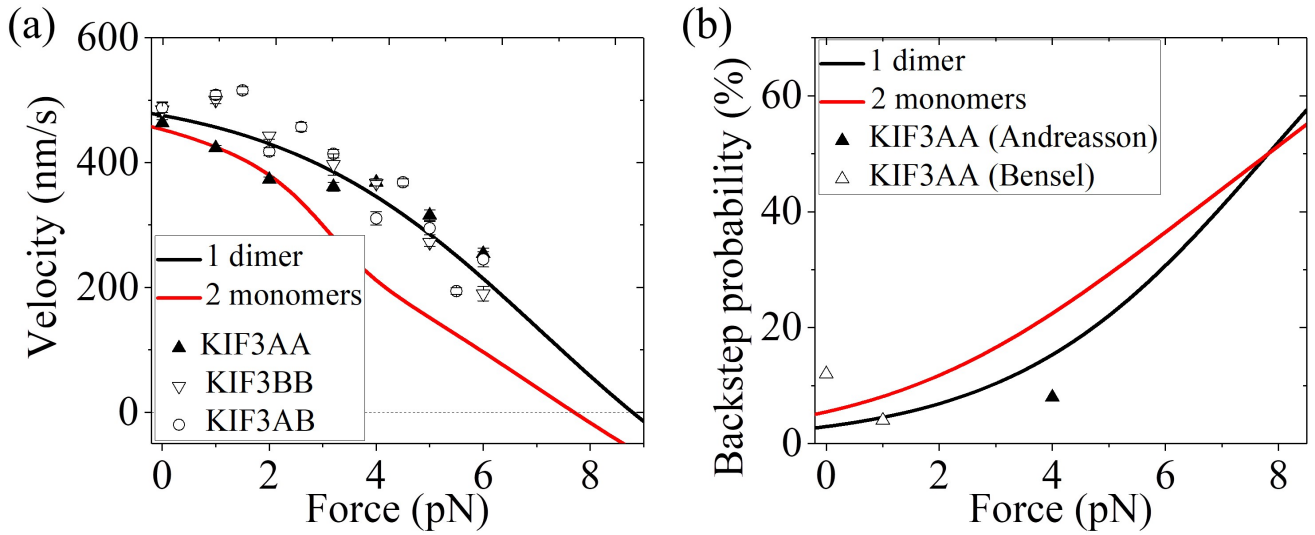


Fig. S2. Results for the dynamics of the cargo transport by the single kinesin-2 KIF3AA, KIF3BB or KIF3AB dimer (black lines) and that by two coupled kinesin-2 KIF3A or KIF3B monomers with the short stalk (red lines). The parameter values are: $k^{(+)} = 64.5 \text{ s}^{-1}$, $k^{(-)} = 0.5k^{(+)}$, $E_0 = 2.9k_B T$ and $\lambda = 0.21$. **(a)** Velocity versus load. Symbols are experimental data from Andreasson et al. [S9]. **(b)** Backstepping probability versus load. Filled symbol is the experimental value (at $F = 4 \text{ pN}$) from Andreasson et al. [S9] measured using the single-molecule optical trapping method. Unfilled symbols are experimental data from Bensen et al. [S10], with the value at $F = 0$ measured using interferometric scattering (iSCAT) microscopy and that at $F = 1 \text{ pN}$ measured using the single-molecule optical trapping method.

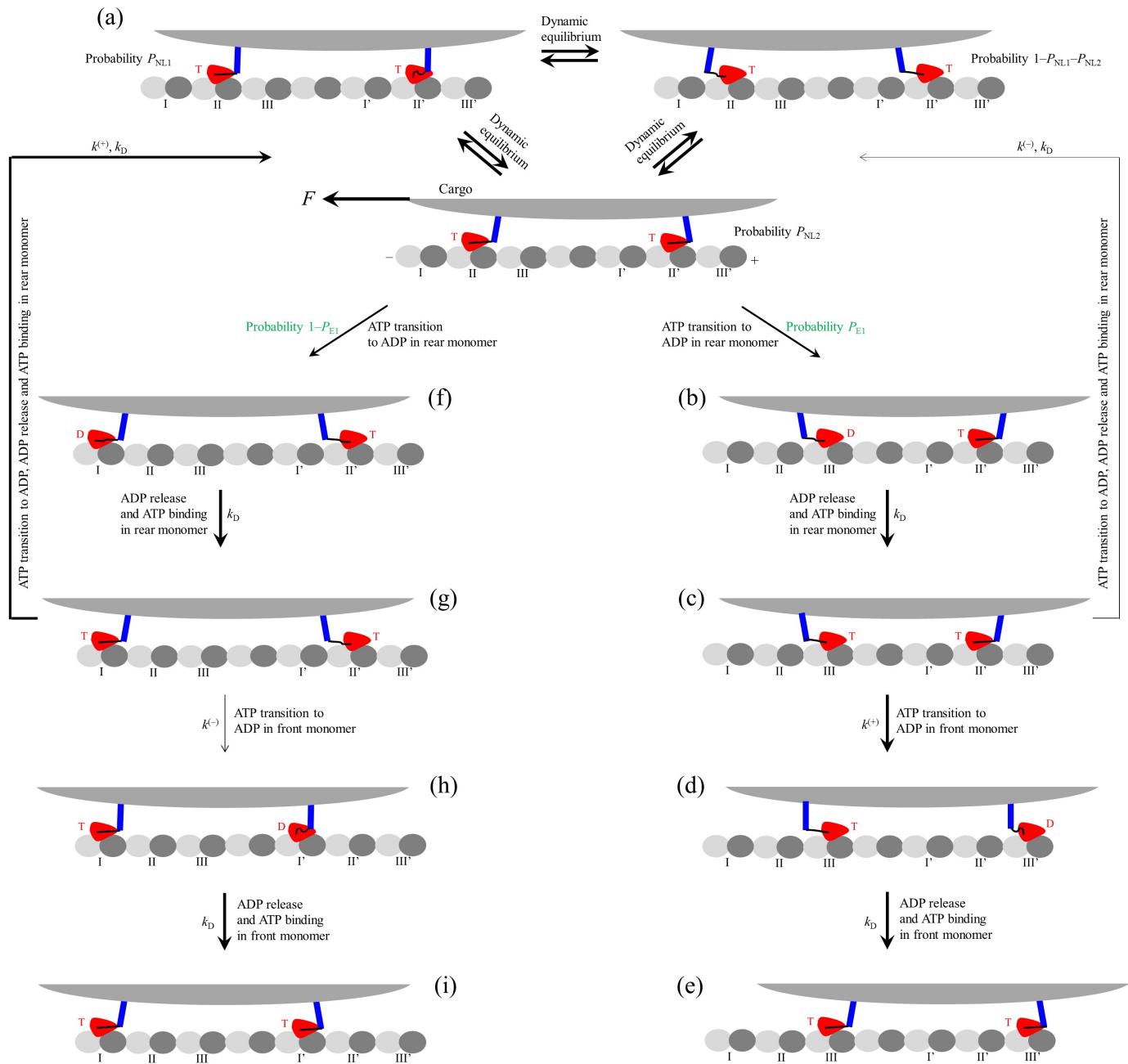


Fig. S3. Schematic illustration of the cargo transport by two coupled kinesin-1 monomers with the short stalk under a backward load F on the cargo for the case of the distance between the two connecting points of the stalk on the cargo being not commensurate to the repeat period of tubulins on the MT filament. (a) – (i) Mechanochemical coupling pathway at saturating ATP concentrations. The description of the pathway is similar to that presented in the main text for the pathway shown in Fig. 1. However, it is noted here that the system in (a) can be in three states: In one state, the two monomers have the docked NL in the forward orientation (lower panel). In another state the rear monomer has the docked NL in the forward orientation and the front monomer has the undocked NL (upper and left panel). In the third state, the two monomers have the undocked NL in the backward orientation (upper and right panel). The three states are in the dynamic equilibrium, with rapid transitions among them. Here, only the transitions following ATP transition

of ADP in the rear monomer in (a) are shown. The thickness of the arrow represents the relative magnitude of the probability of the transition between the two states connected by the arrow. At saturating ATP the rate of ATP binding is considered to be infinitely large. Since ADP release from the monomer bound to MT is a non-rate-limiting step of the ATPase activity, it is considered that ADP release from the ADP-monomer bound to MT occurs before ATP transition to ADP in another monomer with the NL in the forward orientation. Since the diffusion of the monomer from the local tubulin to the adjacent tubulin, which occurs after ATP transition to ADP in the monomer, is on the timescale $< 1 \mu\text{s}$, which is much shorter than the inverse of the rate constant of the ATPase activity, the rate of the diffusion is not indicated here.